Temperature dependence of critical current SIS, SsS, SGS, SNS

SNS proximity thermometer

Metallic contact between a normal metal and a superconductor

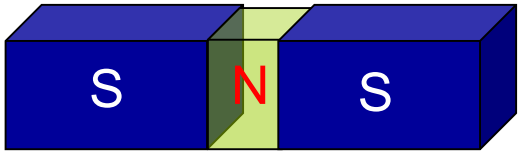

Supercurrent in diffusive SNS junction*:

$$I_J = (1/2eR_n)\int (f(-E)-f(E))j_s(E,\varphi)dE$$

$j_s(E,\varphi)$ – *spectrum of supercurrent carrying states*

Strong temperature dependence of critical current (long junction ($\Delta >> E_{Th}$) and $E_{Th} << k_BT$):

$$I_c \sim T^{3/2}\exp(-(T/T_0)^{1/2})$$

* A.F. Volkov, Phys. Rev. Lett. **74**, 4730 (1995)
* F.K. Wilhelm *et al.*, Phys. Rev. Lett. **81**, 1682 (1998)

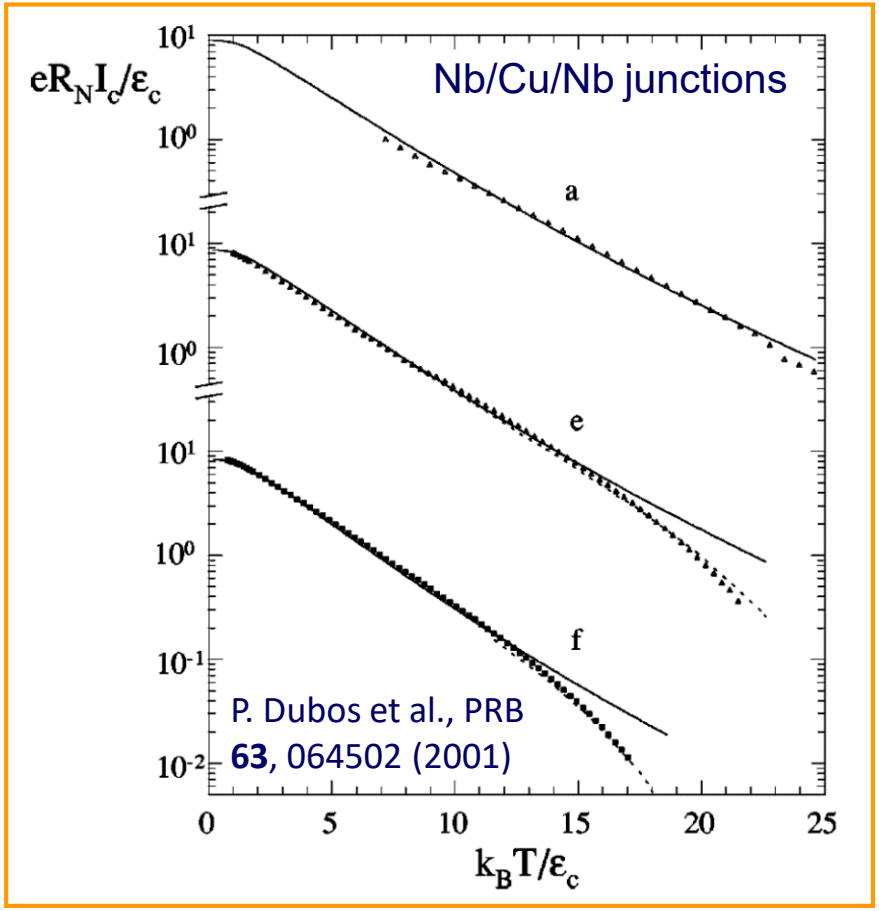

=> Dispersive measurement utilizing Josephson inductance

$$L_j^* = \left(\frac{\Phi_0}{2\pi}\right)^2 \left(\frac{d^2E_0}{d\varphi^2}\right)^{-1}$$

Dispersive Thermometry with a Josephson Junction Coupled to a Resonator (SNS)

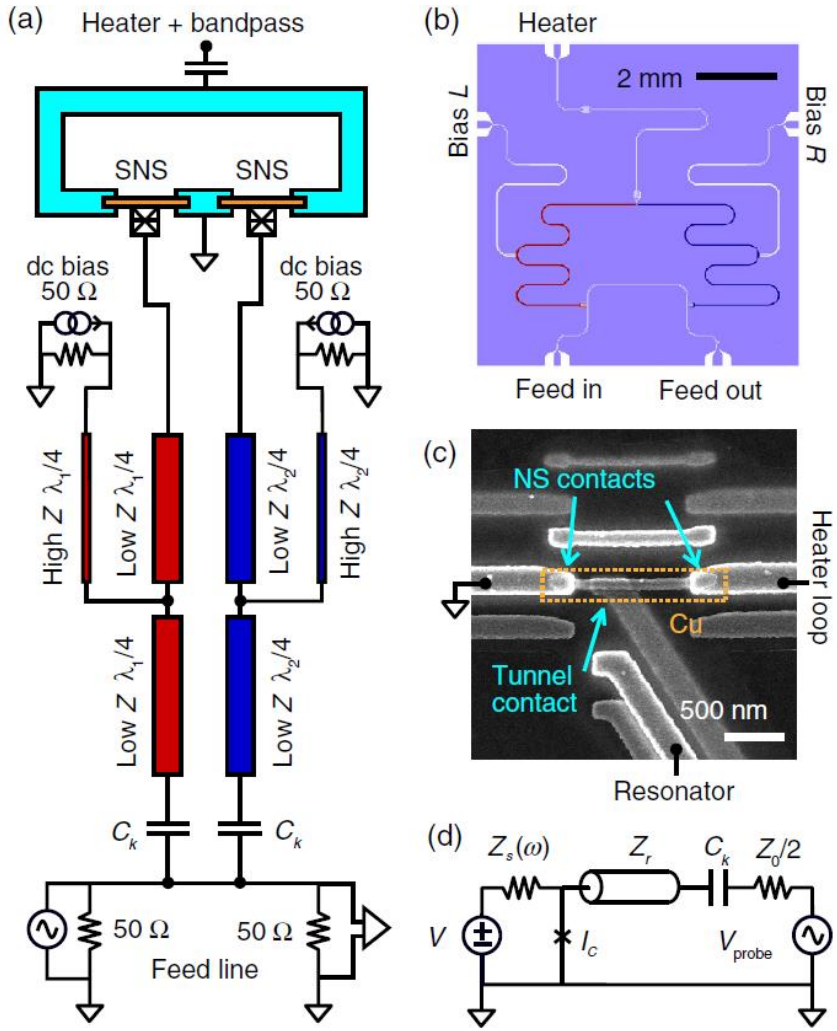

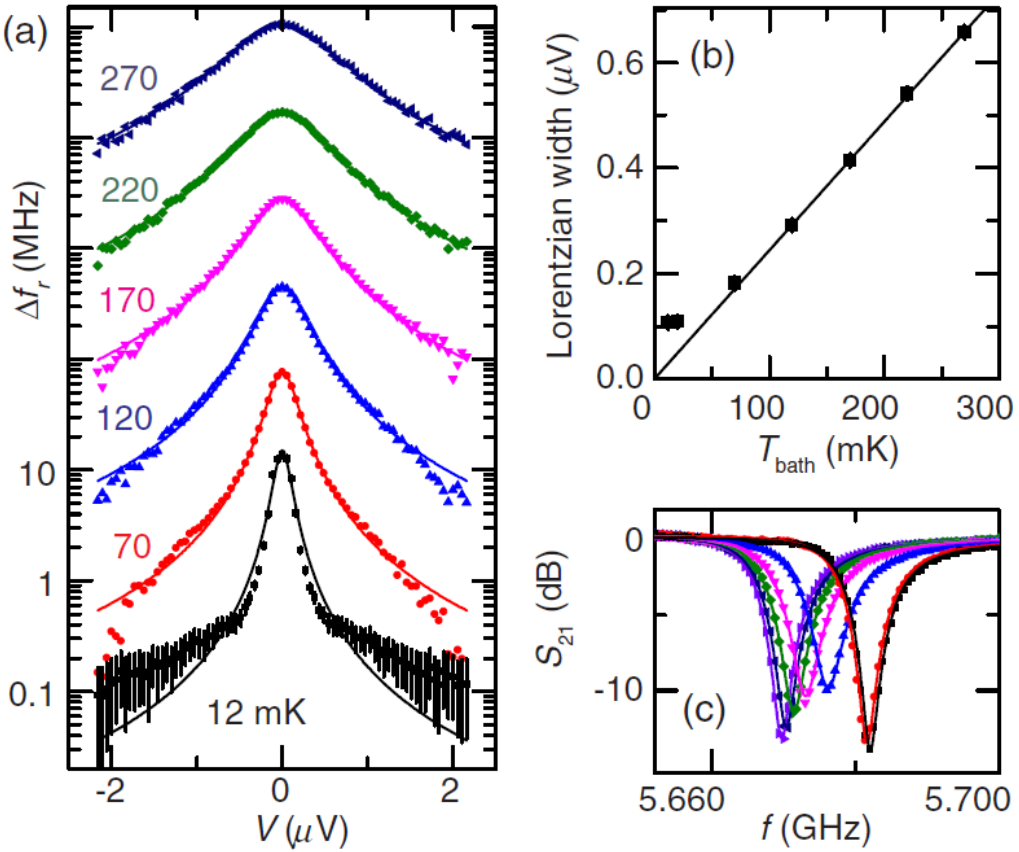

O.-P. Saira, M. Zgirski, K. L. Viisanen, D. S. Golubev, and J. P. Pekola, Phys. Rev. Applied 6, 024005, 2016

Example: Graphene SNS in microwave cavity

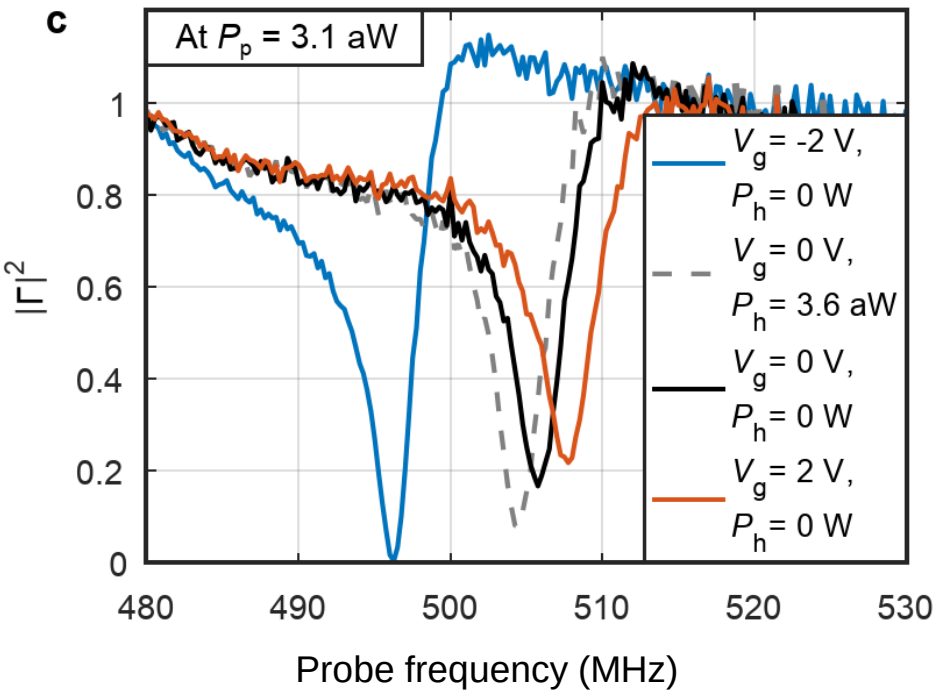

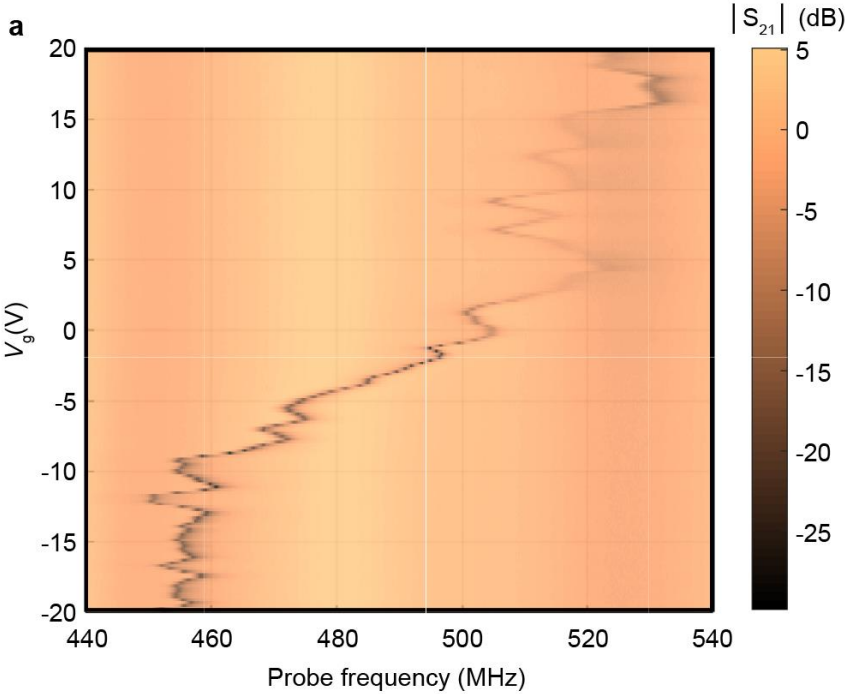

Dirac point around 20 V

Example II: Non-equilibrium state with keeping fixed T_e

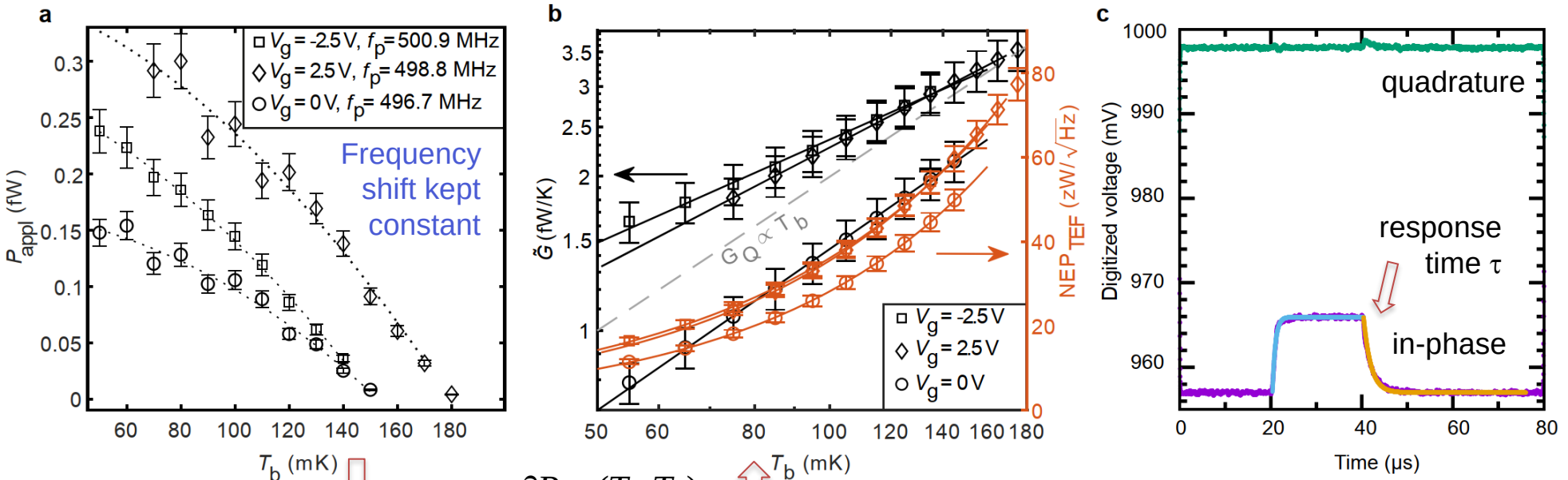

$$\tilde{G} = -\frac{\partial P_{e-b}(T_e, T_b)}{\partial T_B} \qquad \tilde{G} \propto T_b$$

- Photon cooling?
- Electronic diffusion?

Rising edge with τ_r ~100 ns
good for circuit QED read-out

NIS primary Thermometry

Current in NIS tunnel junction:

$$I \simeq I_0 e^{-(\Delta - eV)/k_B T_N} + \frac{\gamma V}{R_T \sqrt{1-(eV/\Delta)^2}},$$

$$I_0 = \sqrt{2\pi\Delta k_B T_N}/2eR_T$$

γ small in good quality junctions

$$V = \frac{\Delta}{e} + \frac{k_B T_N}{e}\ln(I/I_0)$$

$$T_N^B(V) = \frac{e}{k_B}\frac{dV}{d(\ln I)}$$

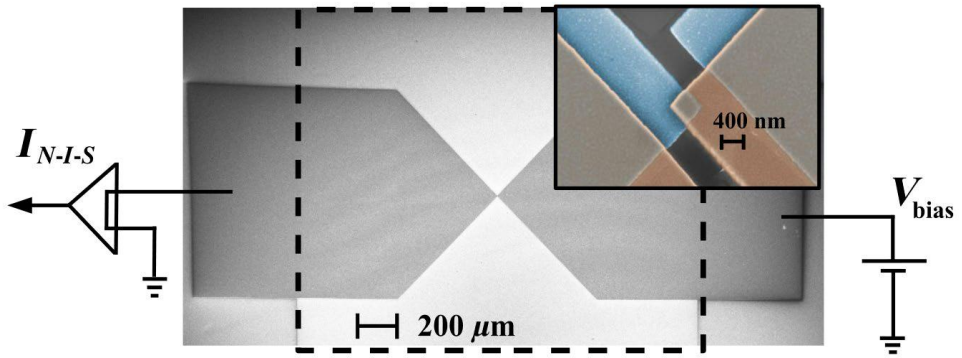

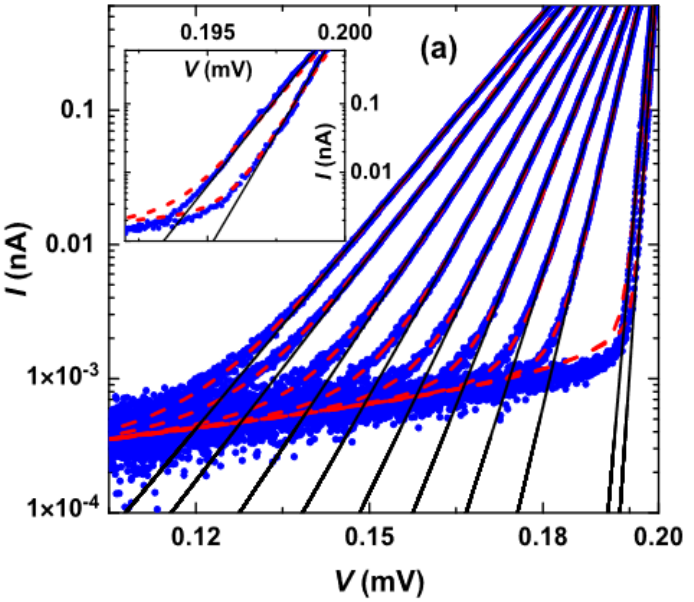

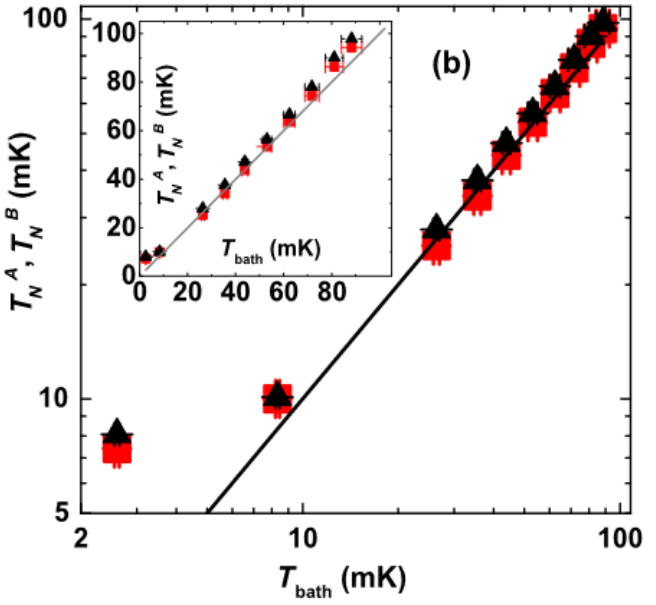

Feshchenko, et al, Phys. Rev. Appl., **4**, 034001 (2015).

Fast temperature readout (NIS thermometer)

Embedding NIS junction in an LC circuit.
RF-NIS readout (20 MHz thermometer, Q=20).

Reflected power from LC circuit (350 MHz):
at resonance => R_{NIS} =>T_e

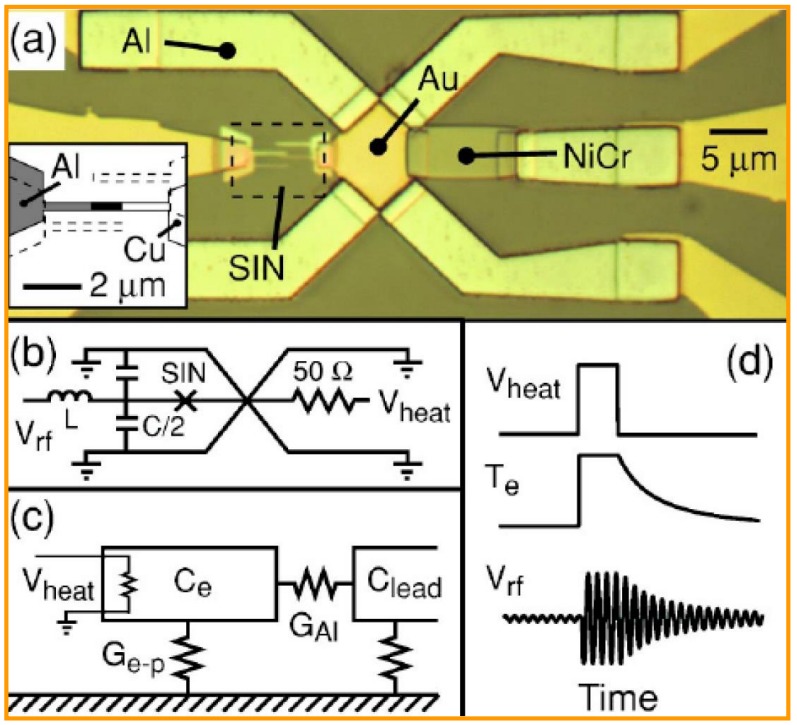

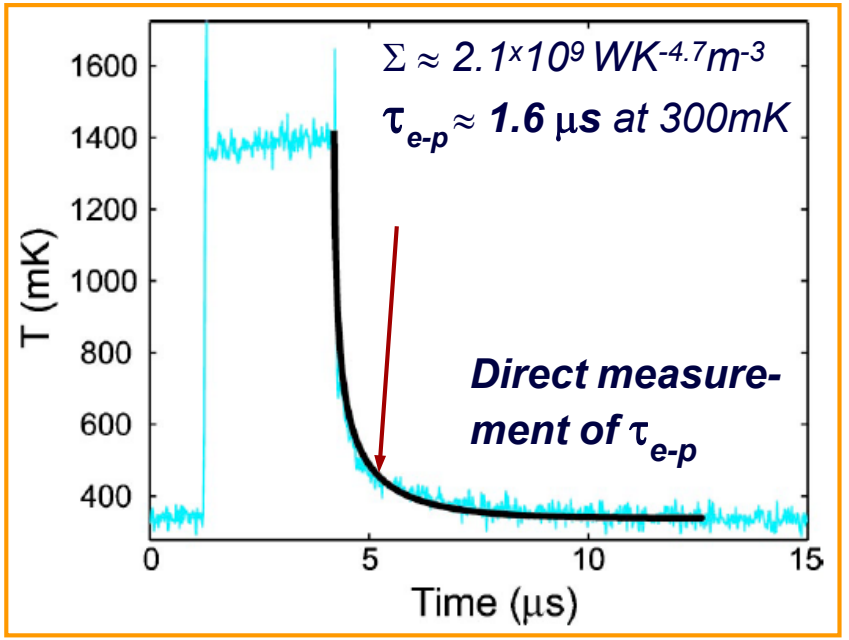

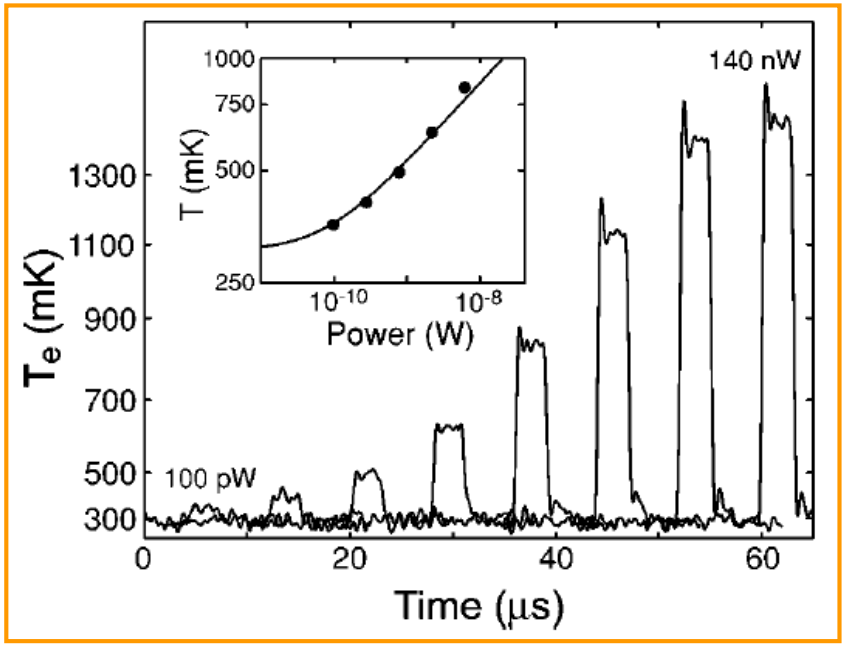

D. R. Schmidt, C. S. Yung, and A. N. Cleland, Phys. Rev. B ***69****, 140301 (2004)*

Fast NIS thermometry for calorimetry

NIS tunnel junction coupled to a resonator with transmission readout $f_0 = 625$ MHz

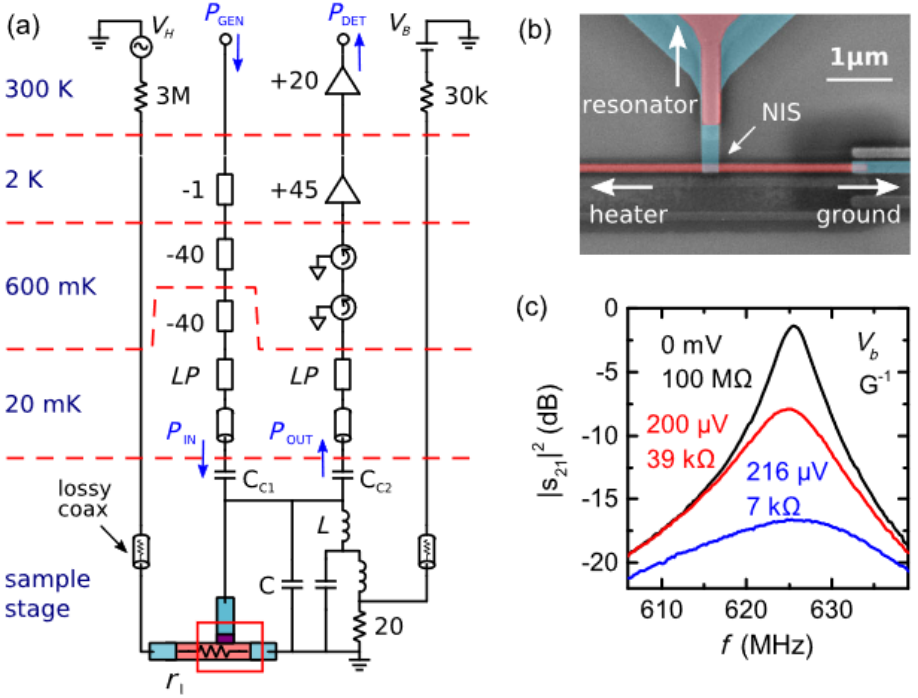

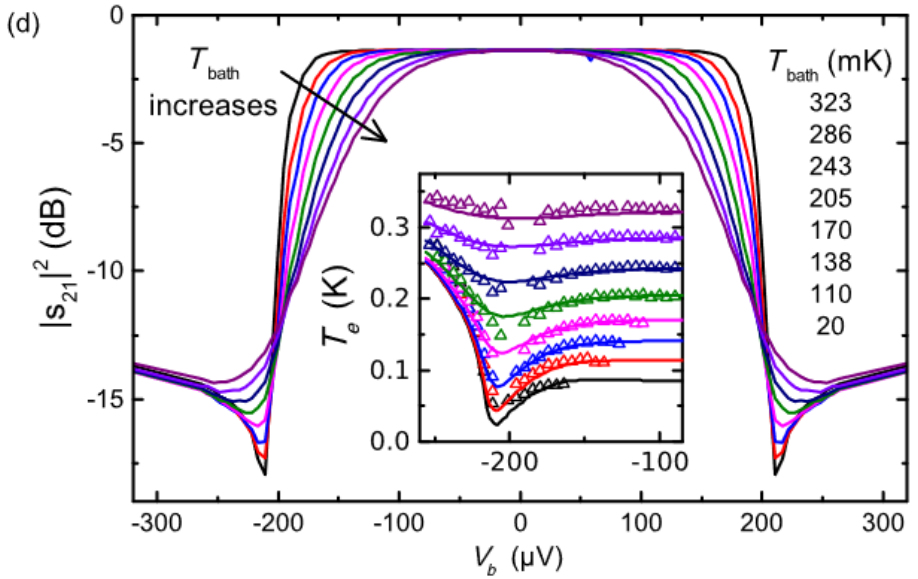

$R_T = 22\ \mathrm{k\Omega}$

Embeded NIS junction in an LC resonant circuit

$$|s_{21}| = 2\kappa \frac{G_0}{G + G_0}$$

$$\kappa = C_{C1}C_{C2}/(C_{C1}^2 + C_{C2}^2)$$

$$G_0 = 4\pi^2 (C_{C1}^2 + C_{C2}^2) Z_0 f_0^2$$

- G_0 for data at $V_b = 0$ and $V_b >> \Delta/e$

$$G = \frac{1}{R_T k_B T_e} \int dE N_S(E) f(E - eV_b)[1 - f(E - eV_b)]$$

S. Gasparinetti et al., Phys. Rev. Appl. **3**, 014007 (2015)

Nanosecond Thermometry with Josephson Junction (SsS)

- Switching current as thermometer
- 10 ns pulses straightforward

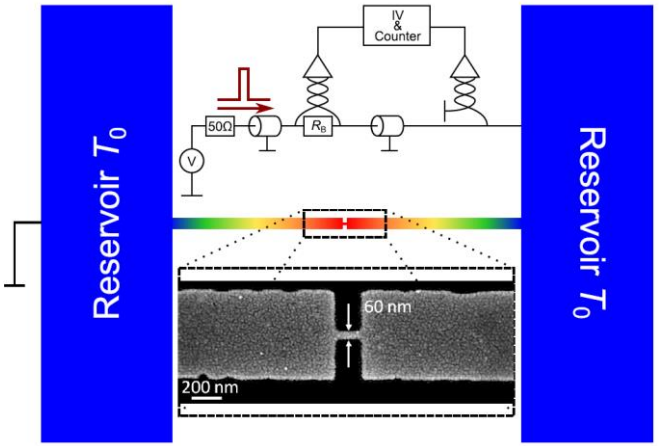

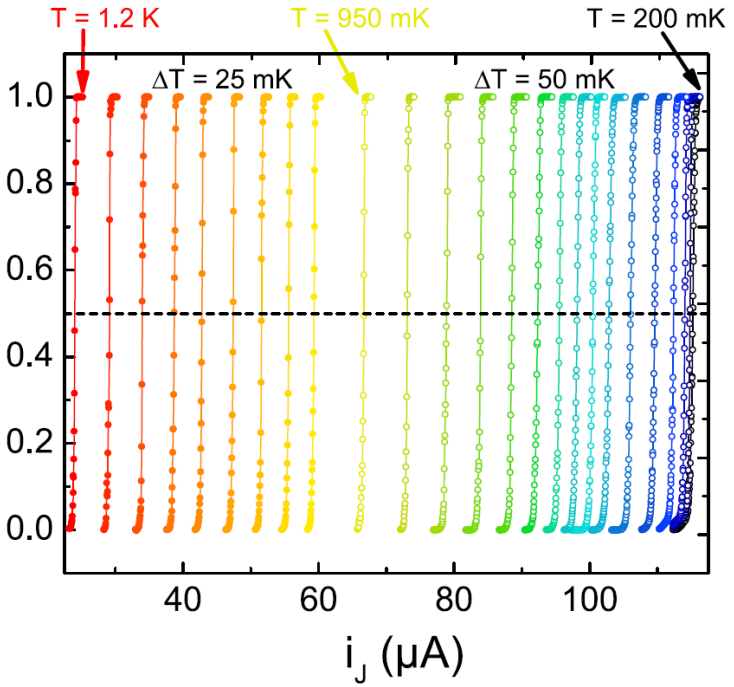

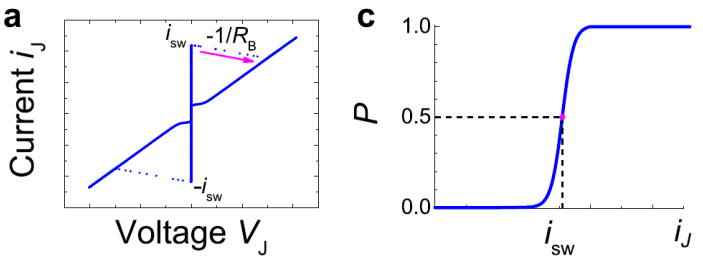

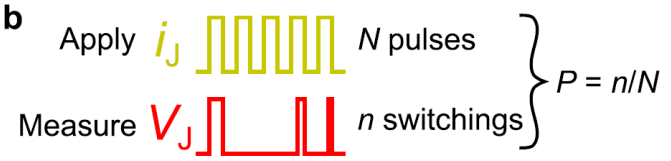

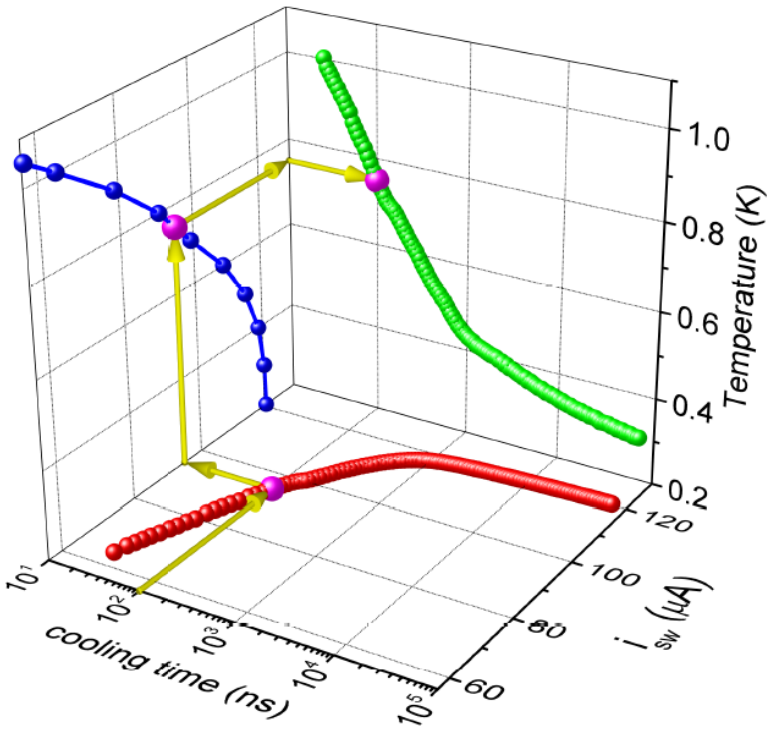

M. Zgirski et al. Phys. Rev. Appl. **10**, 044068 (2018)

Probing of Quasiparticle Diffusion with Nanosecond Resolution

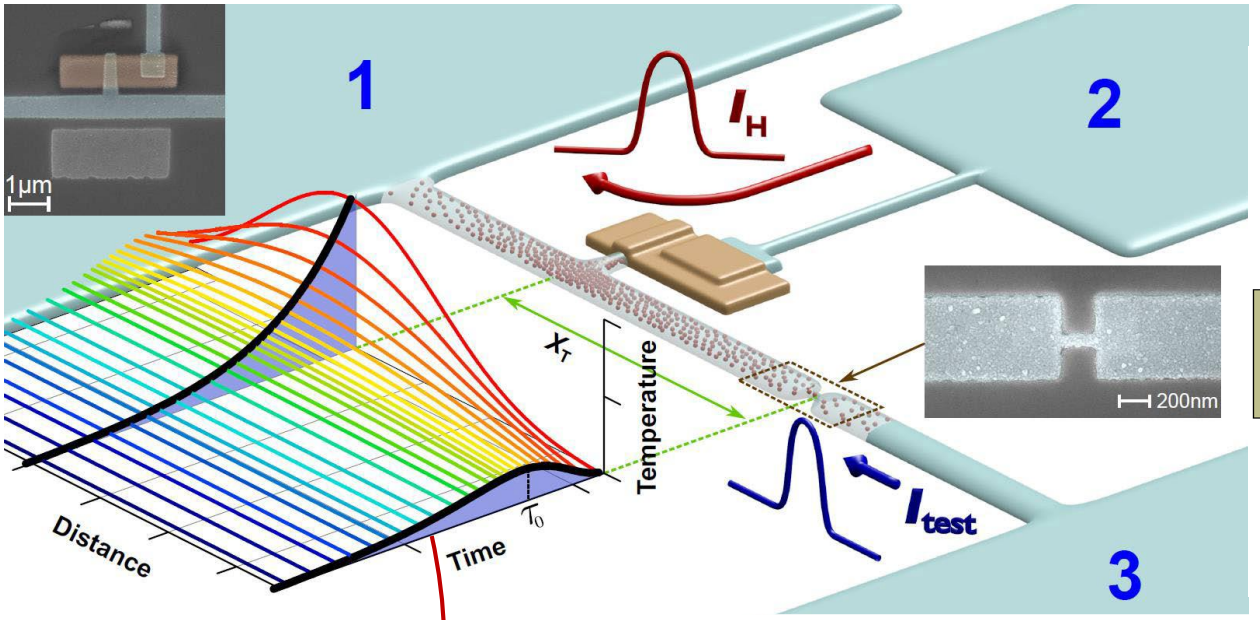

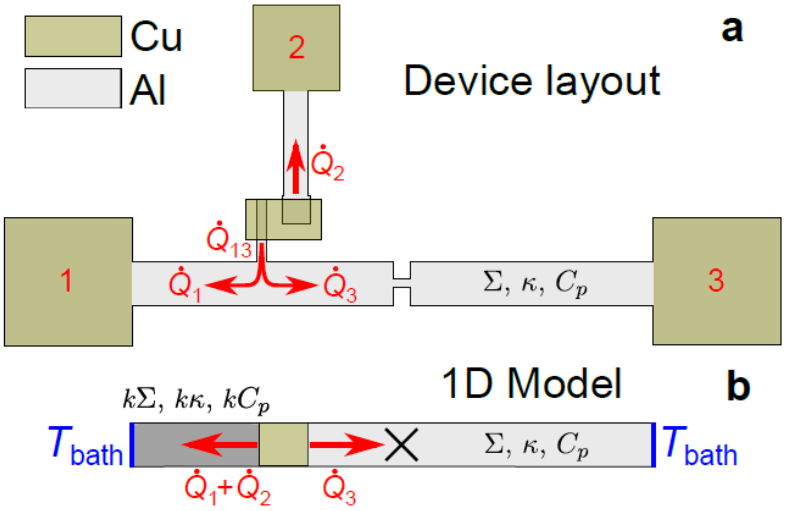

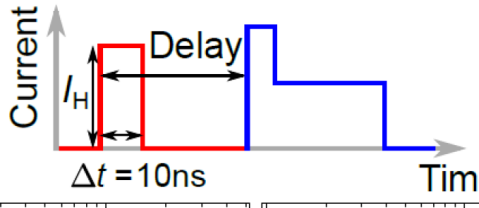

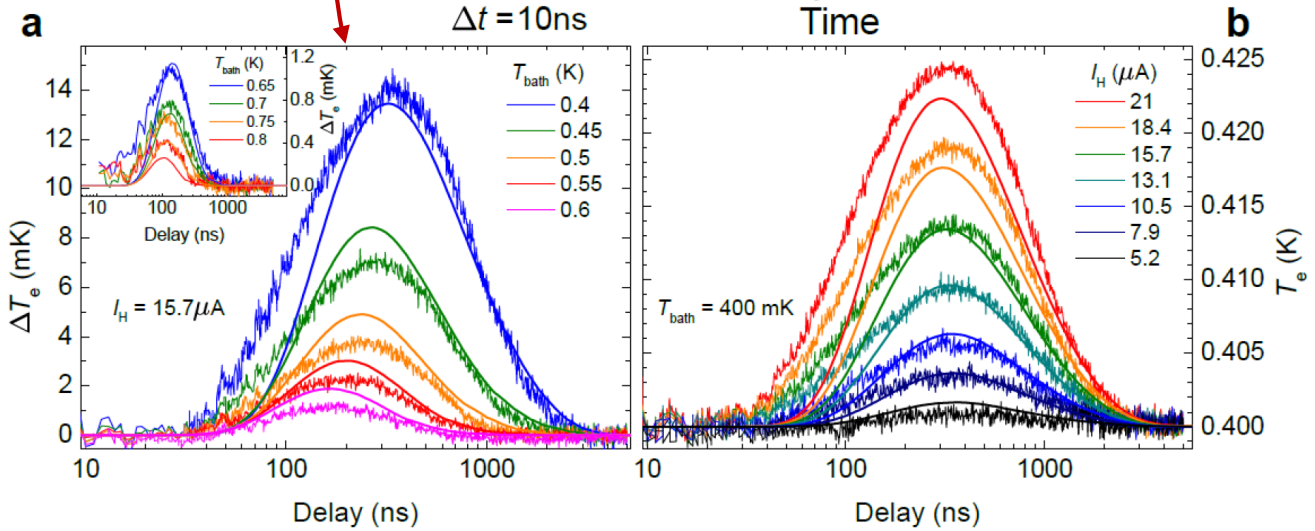

M. Zgirski et al. *Heat hunting in freezer: Direct measurement of quasiparticle diffusion in superconducting nanowire*, *Phys. Rev. Appl.* **14**, 044024 (2020)

Magnetic systems for refrigeration & thermometry

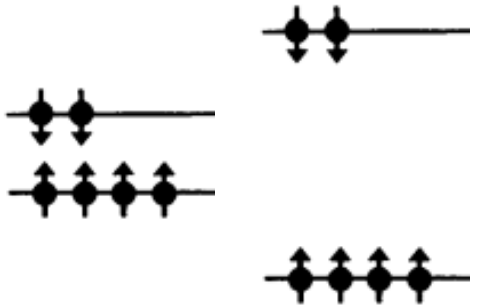

∗ Paramagnetic salts ∗
∗ Hyperfine enhanced systems ∗
∗ Nuclear spins ∗

Boltzmann factor:

e^{-E/k_BT}

– Magnetic moments can be aligned by external magnetic field
– Thermal disorder counteracts the perfect alignment of spins

=>

degree of order (magnetization) depends on the **ratio *B*/*T***

Measure *M* in known *B* and get *T*

OR

Keep *M* constant, so that change in *B* results in change in *T*

=> **refrigeration**

Thermodynamics

Balance between
– magnetic energy: μB $E_{p,m} = -\boldsymbol{\mu} \cdot \mathbf{B}$
– thermal energy: $k_B T$

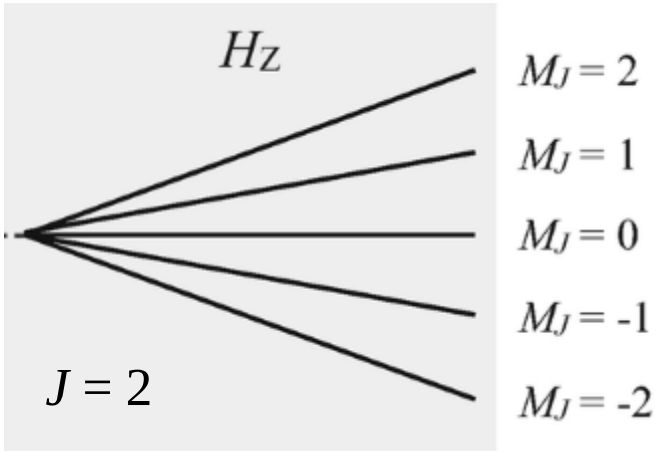

Partition function $Z = \sum_i e^{-\beta E_i}$ $\beta = \frac{1}{k_B T}$

Z for **distinguishable** particles with **spin *J***: $E_m = \frac{m}{J}\frac{\mu B}{k_B T} = \frac{m}{J}x$

Zeeman levels

$$Z = \left[\sum_{m=-J}^{J} e^{-\beta E_m} \right]^N$$

$$Z = \left[\sinh\left(\frac{2J+1}{2J} x \right) \Big/ \sinh\left(\frac{x}{2J} \right) \right]^N$$

Basic relations ...

Entropy: $S = k_B \frac{\partial (T \ln Z)}{\partial T}$ $\qquad Z = \sum_i e^{-\beta E_i}$

Heat capacity: $c_B = T \left(\frac{\partial S}{\partial T} \right)_B$

Magnetization: $M = k_B T \left(\frac{\partial \ln Z}{\partial B} \right)_T$ $\qquad \left(\frac{\partial M}{\partial T} \right)_S = \left(\frac{\partial S}{\partial B} \right)_M$

$$E_s = E_s^{(0)} + \lambda A_s \qquad \langle A \rangle = \sum_s A_s P_s = -\frac{1}{\beta} \frac{\partial}{\partial \lambda} \ln Z(\beta, \lambda).$$

... worked out exactly

$$\frac{S}{R(N/N_A)} = \frac{x}{2J}\coth\left(\frac{x}{2J}\right) - \frac{(2J+1)x}{2J}\coth\left(\frac{2J+1}{2J}x\right) + \ln\left[\frac{\sinh\left(\frac{2J+1}{2J}x\right)}{\sinh\left(\frac{x}{2J}\right)}\right]$$

$$\frac{C_B}{R(N/N_A)} = \frac{x^2}{4J^2}\sinh^{-2}\left(\frac{x}{2J}\right) - \frac{(2J+1)^2x^2}{4J^2}\sinh^{-2}\left(\frac{2J+1}{2J}x\right)$$

$$\frac{M}{\mu N} = \frac{M}{M_{\text{sat}}} = B_J(x) =$$

$$\frac{2J+1}{2J}\coth\left(\frac{2J+1}{2J}x\right) - \frac{1}{2J}\coth\left(\frac{x}{2J}\right)$$

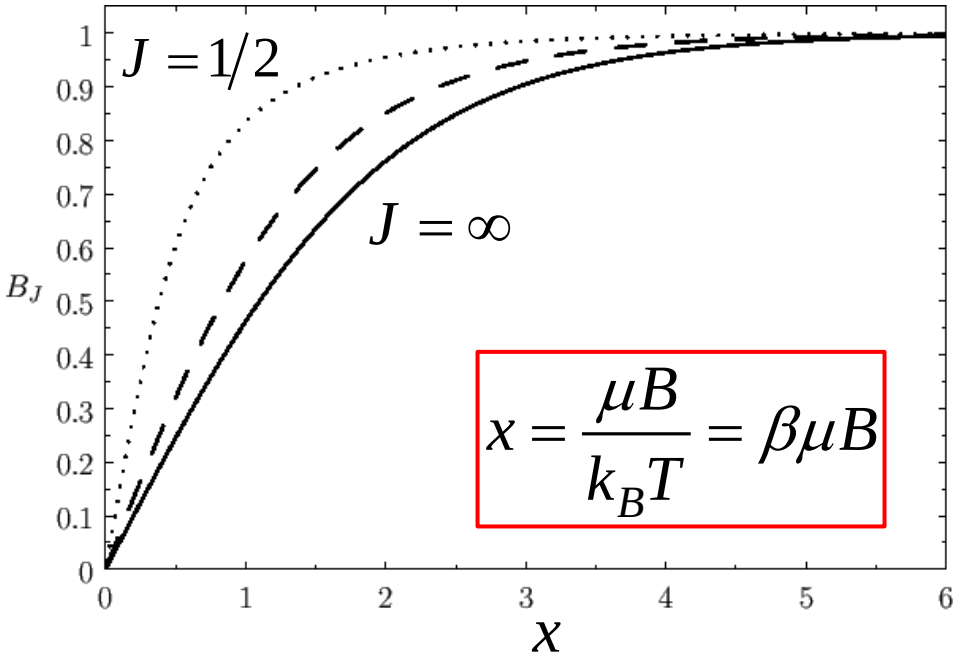

High-T approximations

Often $x << 1$ ($k_B T >> \mu B$) so that it is safe to simplify

$$\frac{S}{R(N/N_A)} \cong \ln(2J+1) - \frac{J+1}{6J}x^2$$

$$\frac{C_B}{R(N/N_A)} \cong \frac{J+1}{3J}x^2$$

$$x^2 \propto \left(\frac{B}{T}\right)^2$$

$$\frac{M}{M_{\text{sat}}} \cong \frac{J+1}{3J}x$$

$$\left(\frac{\partial M}{\partial T}\right)_S = \left(\frac{\partial S}{\partial B}\right)_M$$

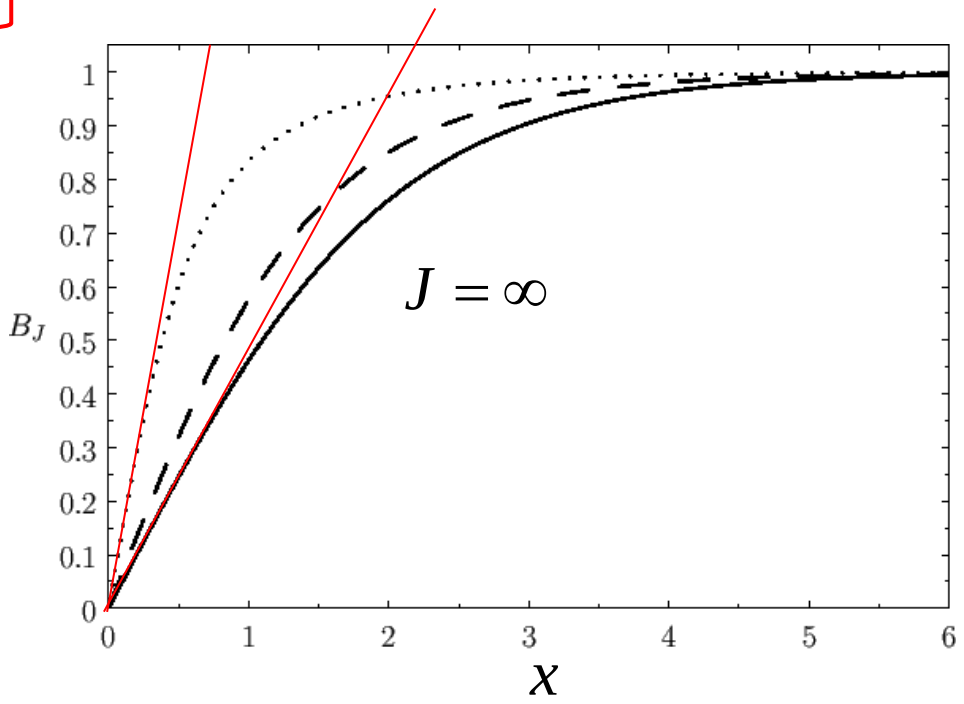

Entropy

All relations above, including molar spin entropy

$$S_n = S/n, \qquad n = N/N_A$$

depend just on the ratio of magnetic field and temperature:

$$S_n = S_n(\boldsymbol{B}/\boldsymbol{T})$$

The limiting value at high temperatures:

$$S_n \underset{T \to \infty}{\longrightarrow} S_{n,\,\max} = R \ln(2J+1)$$

In ***adiabatic processes*** entropy remains constant => T can be made to change in proportion to B. BUT entropy must differ notably from its maximum value to begin with.

Heat capacity

Any magnetic system, regardless of the origin and magnitude of the magnetic moment, **has maximum in the heat capacity**, that depends ONLY on the value of the spin J !

The maximum occurs at

$$\frac{x}{J} = \frac{\mu B}{J k_B T} \approx 1 \ldots 2$$

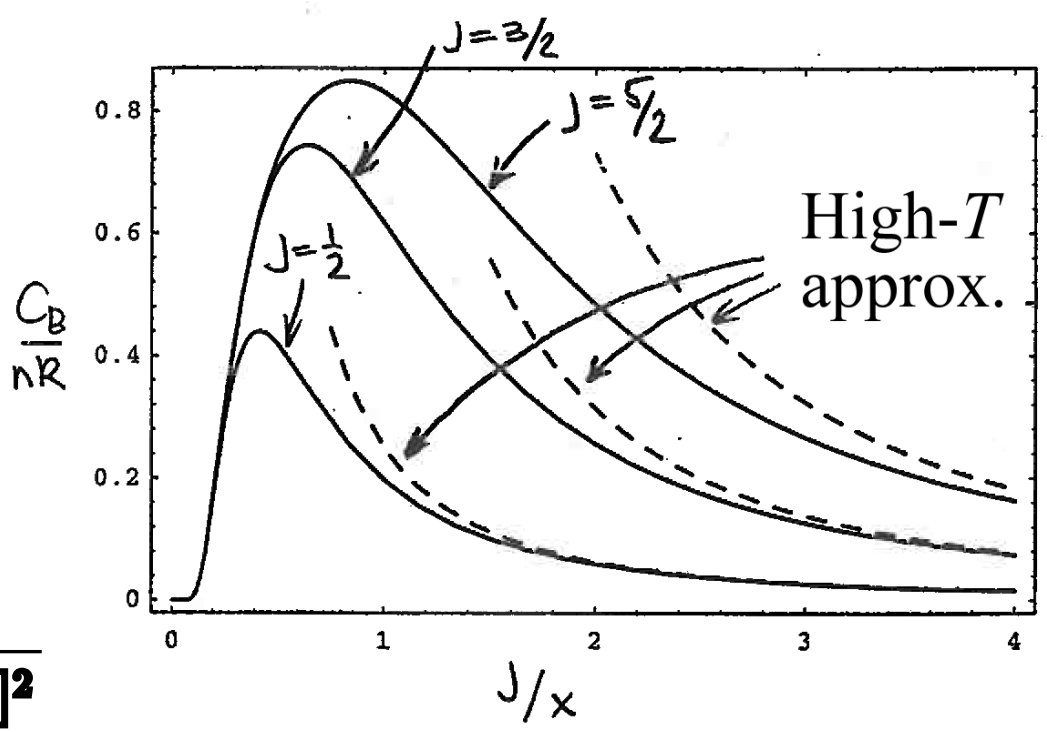

Schottky anomaly in C for two level systems:

$$C_{\text{Schottky}} = R\left(\frac{\Delta}{T}\right)^2 \frac{e^{\Delta/T}}{[1+e^{\Delta/T}]^2}$$

Other related quantities

Susceptibility χ:

$$\chi = \frac{\mu_0 M}{VB} \cong \frac{J+1}{3J} \frac{\mu_0 M_{\text{sat}}}{VB} x = \frac{\lambda}{T}$$

where

$$\lambda = \frac{J+1}{3J} \frac{nR\mu_0}{V} \frac{\mu^2}{k_B^2} = \frac{\lambda}{T} \qquad n = \frac{N}{N_A}$$

is the **Curie constant**, $[\lambda]$ = K

Now, for example

$$C_B \cong \frac{J+1}{3J} nRx^2 = \frac{V\lambda}{\mu_0} \left(\frac{B}{T} \right)^2$$

Internal magnetic field

The spins do not respond to external magnetic field only, they also feel the weak fields of each other. This is represented by the **internal field** $\boldsymbol{b}$.

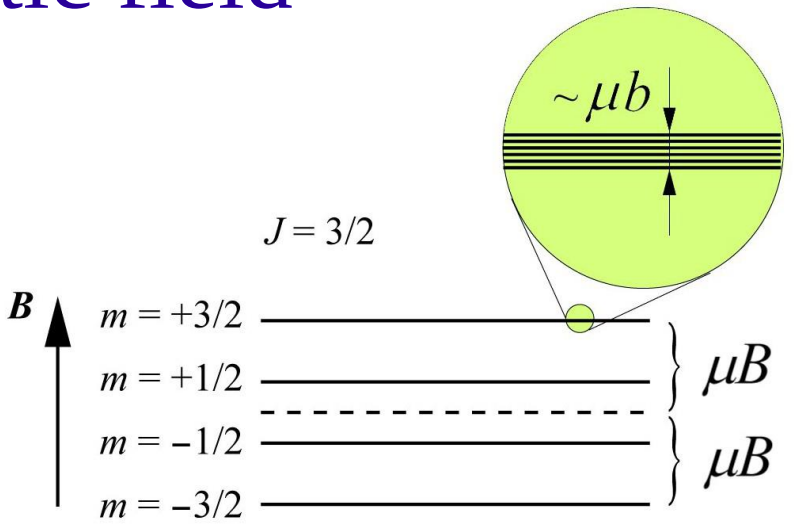

Roughly speaking $\boldsymbol{b \sim k_B T_c / \mu}$,
where T_c is the **magnetic ordering temperature** of the material

This adds quadratically to the external magnetic field:

$$B_{\text{tot}} \approx \sqrt{B^2 + b^2}$$

To have $B_{\text{tot}} \sim B$, one must have rather small b
=> we are interested on materials with low T_c ,
i.e. weakly magnetic materials

Paramagnetic salts

Lowest achievable temperature is limited by magnetic ordering temperature => need weak paramagnets

Weakest known **conventional magnets** (with atomic moments) are so called paramagnetic salts

The magnetic element is buried in an **ionic compound** (salt) containing lots of **crystal water**
e.g. "CMN" $2Ce^{3+}(NO_3)_3 \cdot 3\,Mg(NO_3)_2 \cdot 24\,H_2O$

The moment is due to

- **3d transition elements**
- **4f rare earth metals**

Mn^{2+}, Fe^{3+}, Cr^{3+}, Ce^{3+}, ...

Electronic moments

The unpaired electron at the inner shell of these ions carry a magnetic moment

$$\mu = g\mu_B J \qquad\qquad \boldsymbol{\mu} = -g_J \frac{\mu_\mathrm{B}}{\hbar}\boldsymbol{J}$$

with Landé factor

$$g = \frac{3}{2} + \frac{S(S+1) - L(L+1)}{2J(J+1)}$$

and the Bohr magneton

$$\mu_B = \frac{e\hbar}{2m_e} \approx 9.27 \cdot 10^{-24}\ J/T$$

Useful compounds

The strength of the magnetic interactions is controlled by the distance between the moments: $T_c \sim \mu^2/r^3$

The larger moment, the smaller magnetic field is sufficient

	compound	T_c/K	
"MAS"	$Mn^{2+}\,SO_4 \cdot (NH_4)_2SO_4 \cdot 6\,H_2O$	0.17	
"FAA"	$Fe^{3+}{}_2\,(SO_4)_3 \cdot (NH_4)_2SO_4 \cdot 24\,H_2O$	0.03	ferric ammonium alum
"CPA"	$Cr^{3+}{}_2\,(SO_4)_3 \cdot K_2SO_4 \cdot 24\,H_2O$	0.01	chromium potassium alum
"CMN"	$2Ce^{3+}\,(NO_3)_3 \cdot 3\,Mg(NO_3)_2 \cdot 24\,H_2O$	0.002	

Cerium can be **further diluted** by nonmagnetic lantanum => LCMN (used in thermometry)

Entropy curves of paramagnetic salts

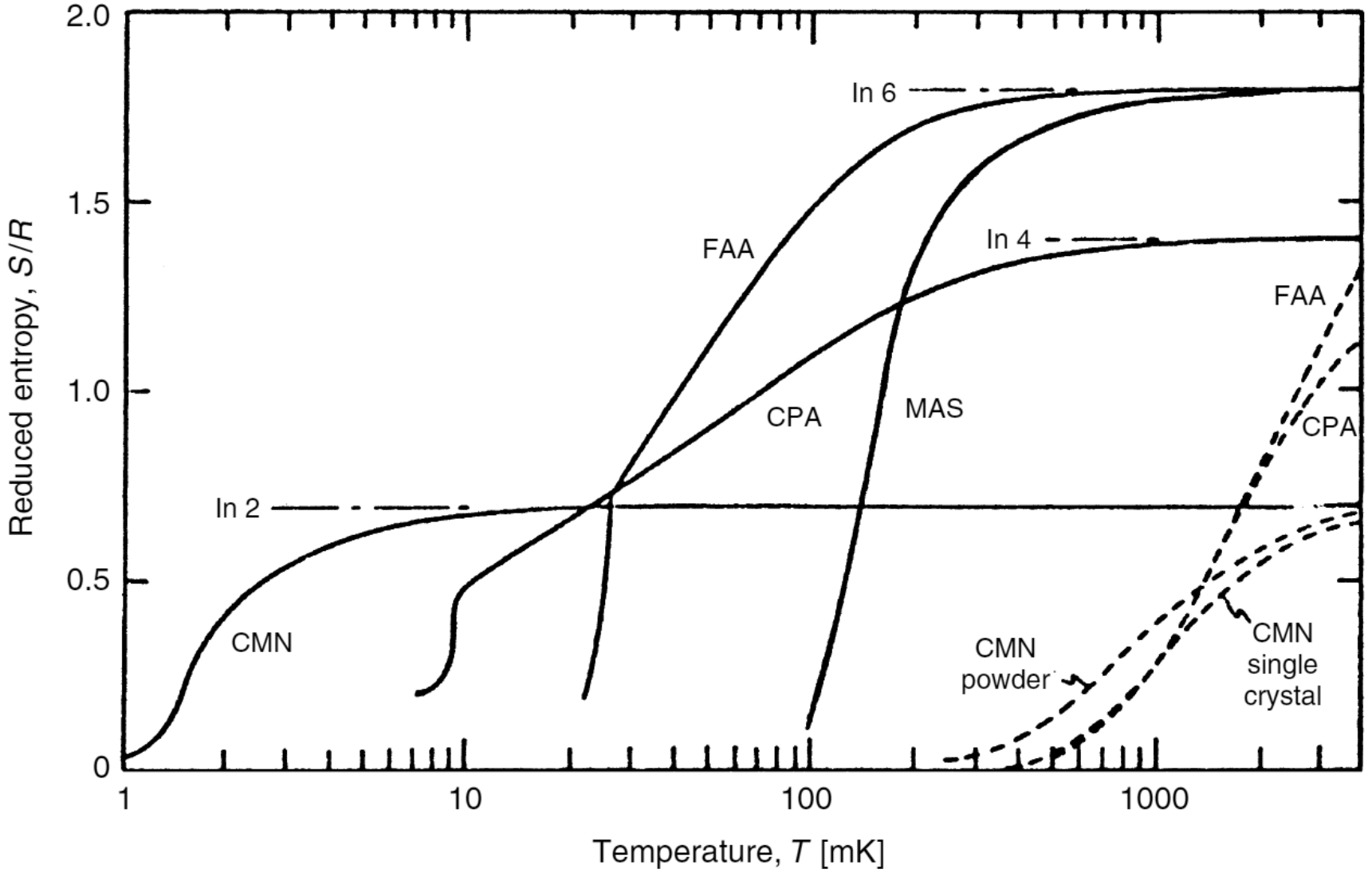

Fig. 9.2. Entropies S (divided by the gas constant R) of four salts suitable for paramagnetic demagnetization as a function of temperature in zero field (———) and in 2 T (– – –). (For the chemical formula of the salts see the text.)

Conventional magnetic thermometry

Measure the **magnetization** $M \cong \frac{V\lambda}{\mu_0}\frac{B}{T}$ ($M << M_{sat}$)

or magnetic **susceptibility** $\chi = \frac{\mu_0 M}{VB} \cong \frac{\lambda}{T}$ (Curie's law)

or **dynamic magnetic susceptibility** $\chi_d = \frac{\mu_0}{V}\frac{dM}{dB} \approx \frac{\lambda}{T} \approx \chi$

In order to operate at mK-range, B must not be very large
=> **internal field *b* is significant**

Effective magnetic fields

It is useful to distinguish three different contributions to B_{tot}:

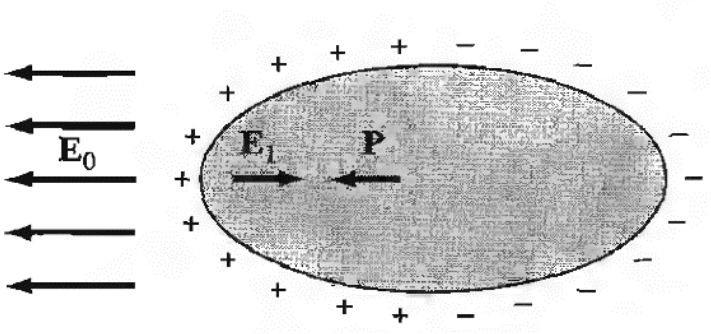

– external magnetic field B_{ext}
– **Weiss field** $\boldsymbol{B_W}$ due to spin-spin interactions
– demagnetization field B_d depending on the sample shape

$$\boldsymbol{B_{tot} = B_{ext} + B_d + B_W} \qquad E_{\text{tot}} = E_{\text{ext}} + E_1 + P$$

Demagnetization field $\boldsymbol{B_d = -D\mu_0 M/V}$ can be written in terms of the demagnetization factor D which is for

– sphere: $\boldsymbol{D = 1/3}$
– plane $\perp$ $\boldsymbol{B}$**:** $\boldsymbol{D = 1}$
– plane $\parallel$ $\boldsymbol{B}$**:** $\boldsymbol{D = 0}$

Effective magnetic fields (cont.)

Weiss field $B_W = (\alpha + R)\mu_0 M/V$ depends on the lattice symmetry and on the **exchange interaction** between the spins

- **for cubic crystals $\alpha = 1/3$**
- **exchange parameter R** can be positive or negative (ferro- or antiferromagnetic exchange)

For a specific sample $B_{tot} = B_{ext} + (\Delta/\lambda)\,\mu_0 M/V$

with $\Delta/\lambda = \alpha + R - D$

Curie-Weiss law

Spins adapt to **total field**: $\chi_{\text{spin}} = \dfrac{\mu_0 M}{V B_{\text{tot}}}$

$$\Rightarrow \quad M = \frac{V\chi_{\text{spin}}}{\mu_0}\left(B_{\text{ext}} + \frac{\Delta\mu_0}{\lambda V} M\right) = \frac{V\chi_{\text{spin}} B_{\text{ext}}}{\mu_0}\left(\frac{1}{1-\Delta\chi_{\text{spin}}/\lambda}\right)$$

Measured susceptibility $\chi_d = \dfrac{\mu_0}{V}\dfrac{dM}{dB_{\text{ext}}} = \dfrac{\chi_{\text{spin}}}{1-\Delta\chi_{\text{spin}}/\lambda}$

$\chi_{\text{spin}} = \lambda/T \Rightarrow \chi_d = \dfrac{\lambda/T}{1-\Delta/T} = \dfrac{\lambda}{T-\Delta}$ with $\boldsymbol{\Delta/\lambda = \alpha + R - D}$

Ferromagnetism $\Delta > 0$
Antiferromagnetism $\Delta < 0$
} (here $\boldsymbol{\alpha - D = 0}$)

Inverse susceptibility vs. T

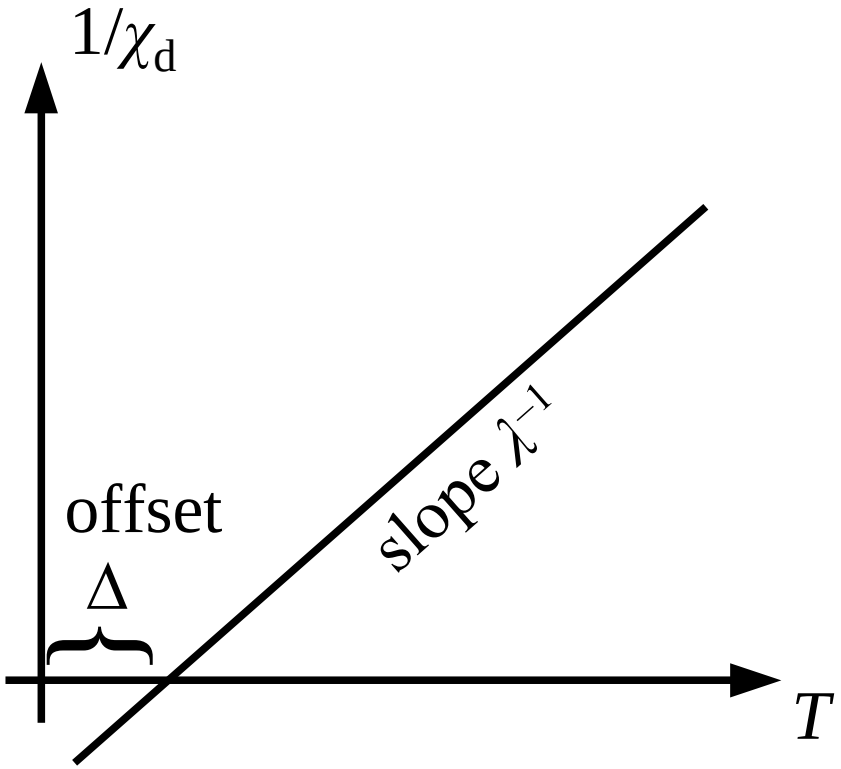

$$\chi_d^{-1} = \left(\frac{\lambda}{T-\Delta}\right)^{-1} = \frac{1}{\lambda}(T-\Delta)$$

positive Δ : ferromagnet
negative Δ : antiferromagnet

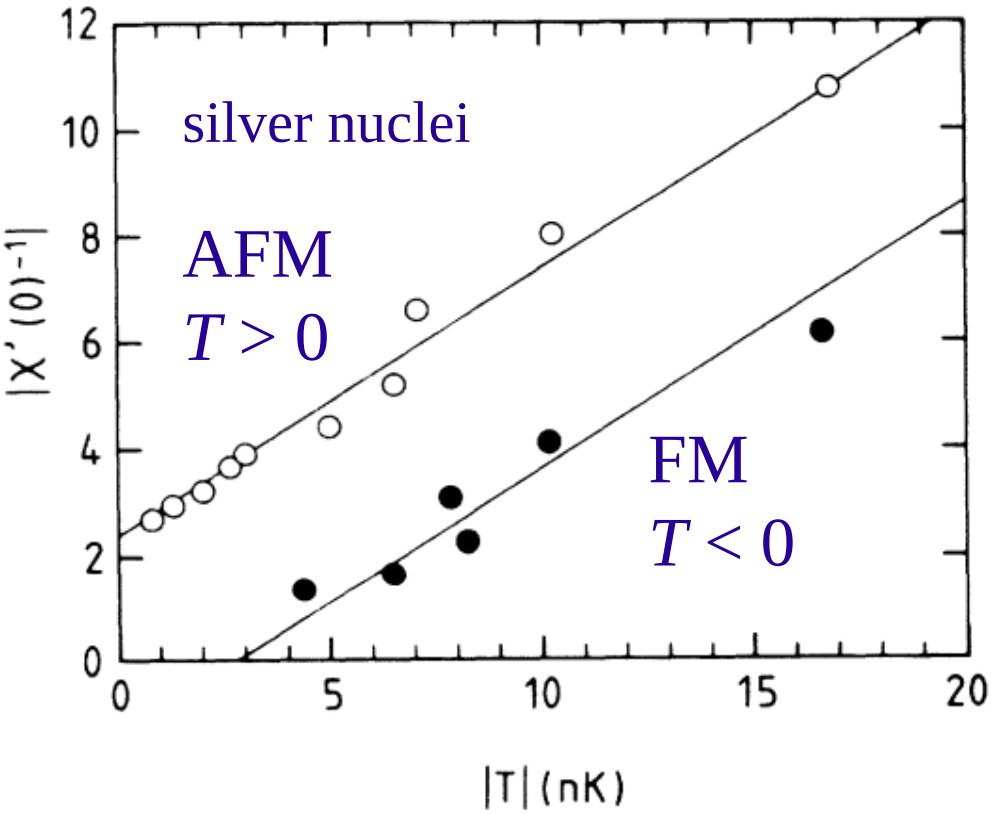

P.J. Hakonen, S. Yin, O.V. Lounasmaa, Phys. Rev. Lett. **64**, 2707 (1990)

Maximum entropy state

$T > 0$: free energy minimum
$T < 0$: free energy maximum

CMN (or LCMN) thermometers

These salts are insulators => exchange is weak => $R << 1$
It is a good idea to make the **sample nearly spherical**

For example cylinder with $L \sim d$ => $D \sim 1/3$
Then $\alpha + R - D \sim 0$ => Curie behavior $\chi \sim \lambda/T$
Typically $|\Delta| \sim 0.1 \ldots 1$ mK

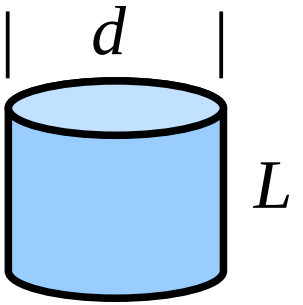

Limiting factor is often poor **thermal contact** to the sensor
– thin **silver wires** or foils are usually mixed in with the salt
– powdered salt can be used to **measure *T* of helium liquids**

Chemical stability (**dehydration**) may be another problem
– has to be recalibrated in each cooldown

Some realizations

Gradiometric arrangement improves sensitivity of the measurement

Fig. 12.37. Schematic of setups for paramagnetic thermometry

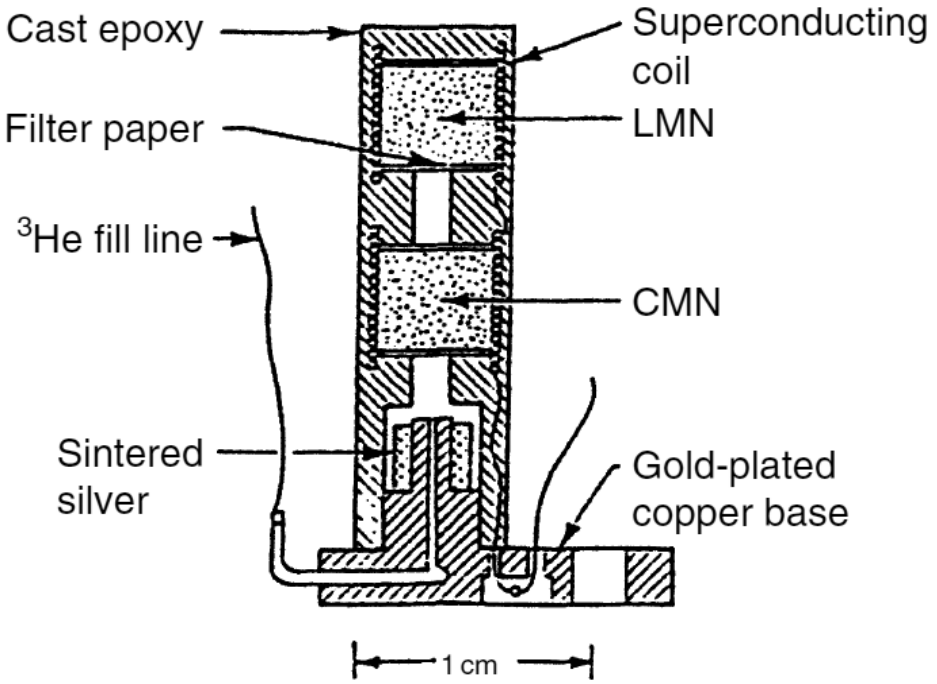

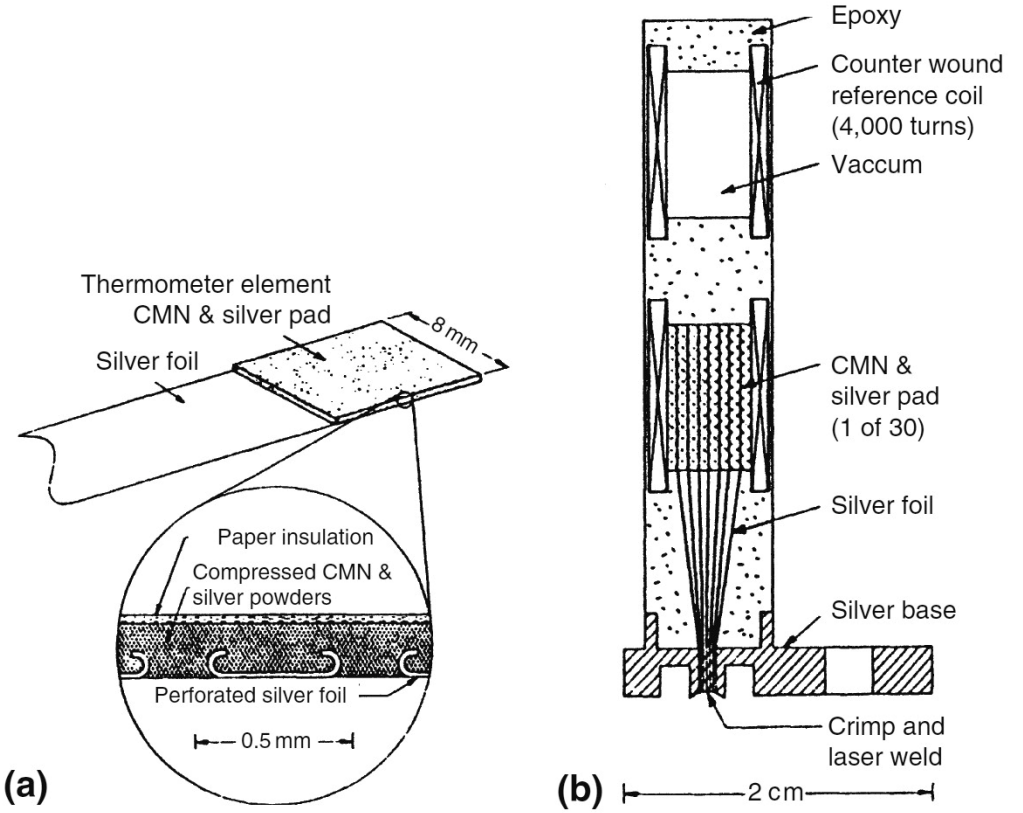

Fig. 12.39. Single element (**a**) and completed design (**b**) of the CMN thermometer

Measuring schemes

Measuring field (B = 0.1 ... 10 mT) must have extremely good stability

=> **superconducting shields & nonmagnetic construction**

– relatively easy and quick method

– simple relationship with T

– needs **a single point for calibration**

– sensitivity improves towards low T

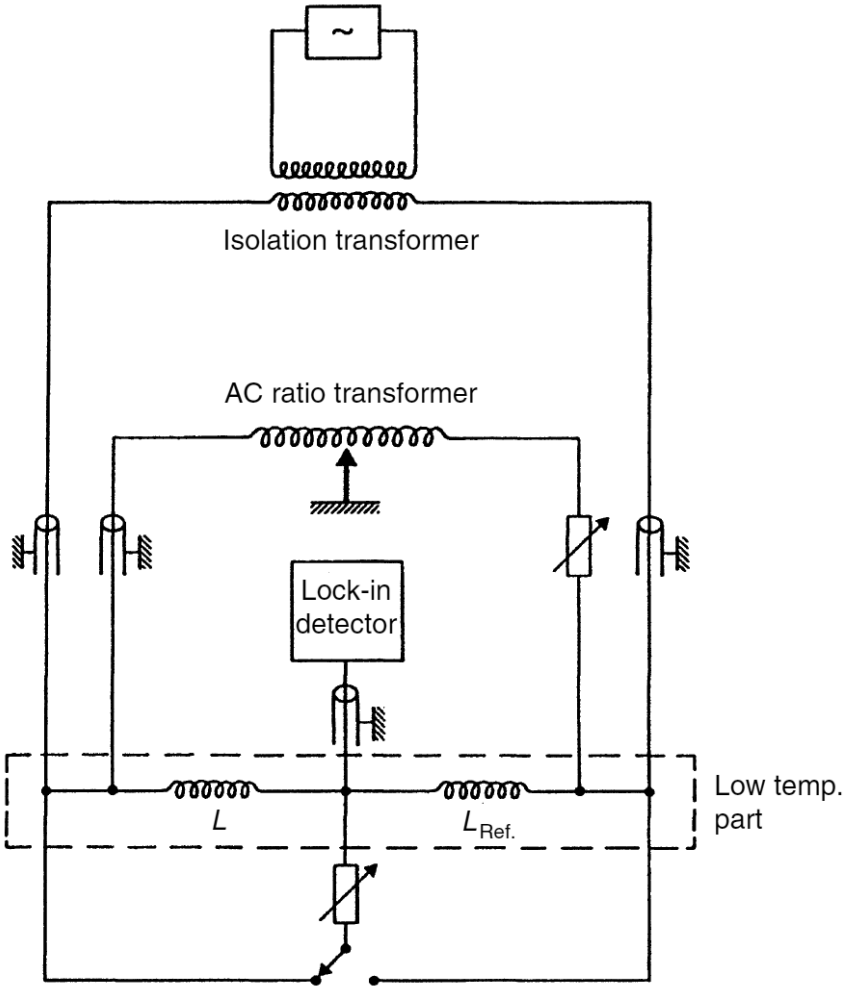

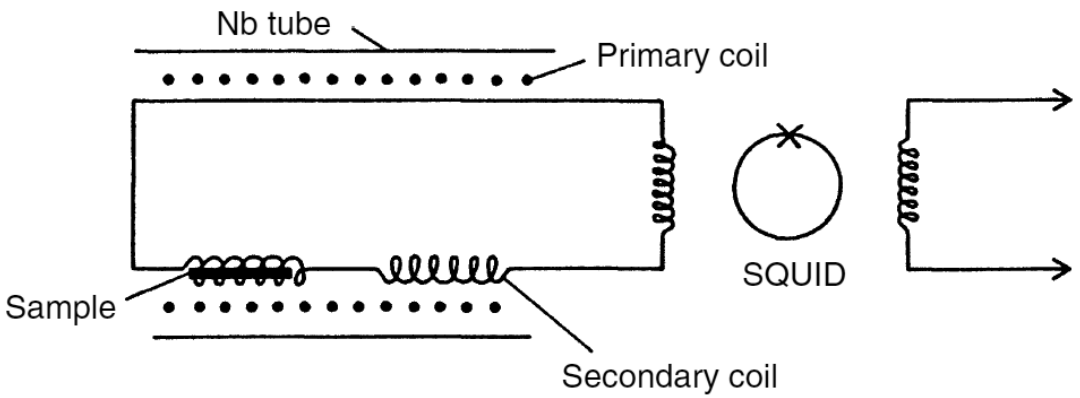

Combined with SC fixed point device

– Superconducting transition points provide calibration points
– CMN thermometer interpolates/extrapolates from these

SRD1000 superconductive reference device

- The device supports 10 reference temperatures T_C between 10 mK and 1.2 K provided by the superconductive transitions of samples of various materials
- A compact array of planar micro-coils detects the transitions
- A Cryoperm / niobium shield and a compensation coil reduces ambient magnetic fields by a factor of 400
- Filters suppress the effects of RF-interference
- Evaluation by various metrological institutes in Europe has proven that the SRD1000 concept is reliable for transferring the PLTS-2000
- The typical uncertainty levels of determining the T_C 's range from about 0.04 mK at 15 mK to about 0.8 mK at 1.2 K

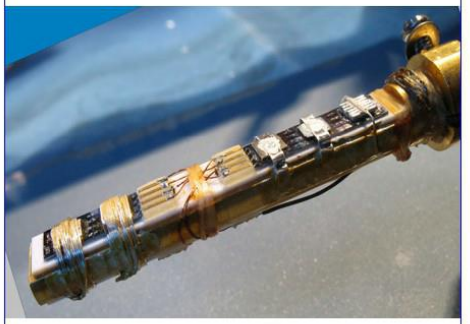

Detector array with reference samples

CMN thermometer option

- The optional CMN thermometer fully integrates with the SRD sensor unit and the MIDS-202 detection electronics
- It provides continuous thermometry in the range of <10 mK to 4 K
- Reading are reliable due to the 'on board' calibration points of the SRD sensor unit
- The resolution is better than 0.5 mK for T < 0.5 K and better than 0.5 % for 0.5 K < T < 1 K

Combined SRD and CMN sensor block

Impurity paramagnetism

Foreign magnetic atom (e.g. Fe) can **polarize the paramagnetic host** with large permeability (e.g. Pd) => giant moment ~ 10 μ_B

Few ppm of Fe in Pd gives reasonable magnetization to measure

Moment density is low
& randomly located =>
no magnetic order

Random moment distribution
results in **spin-glass transition**
at $T_g \sim 0.1\ \text{mK}\ x_{\text{Fe}}/\text{ppm}$

Above T_g: $\chi \propto 1/T$

Below T_g: $\chi \propto T$

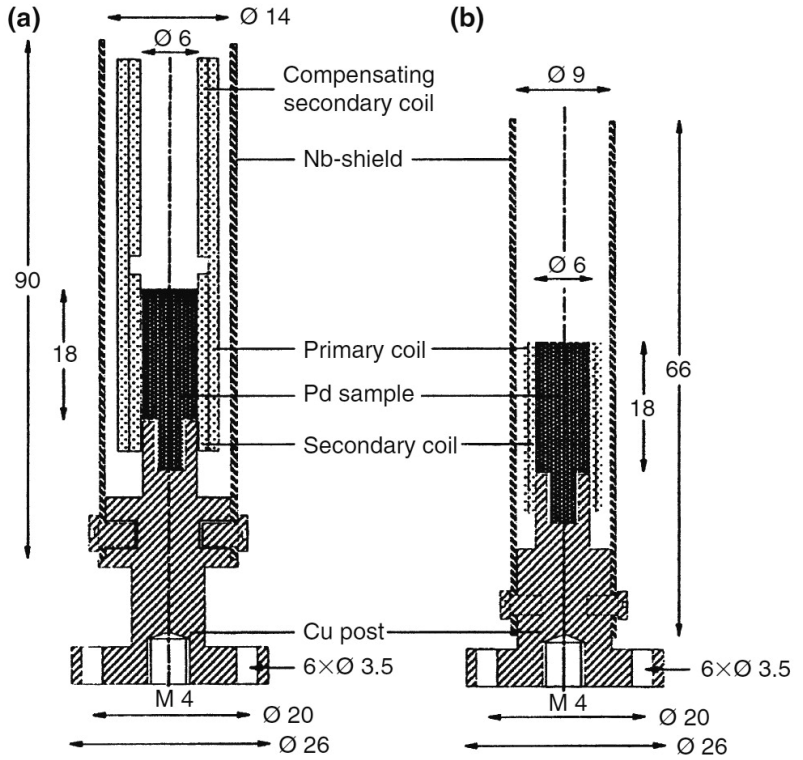

Fig. 12.41. Design of *Pd*Fe susceptibility thermometers. (**a**) With compensated secondary coils; (**b**) without compensated secondary coils. Dimensions are given in mm. The sample is a palladium rod containing 10–30 ppm Fe. Slits should be cut into the Pd rod to reduce eddy-current heating.

Magnetic refrigeration

- Initial condition with **low entropy** $S = S_i < S_{max}$, ($\Delta S/S_{max} > 0.2$)
  has to be prepared by high field B_i / low temperature T_i
- **No other entropy** in the system should be comparable to this
- The system must be made isolated (**adiabatic**); **heat switch** needed
- The magnetic field must be changed reversibly (i.e slowly enough)
  => corresponding change in temperature (B/T **= const.**)
- **The weaker the magnetic system, the larger** B_i/T_i **is needed**

BUT the lower final temperature is achievable, as $B_{min} \sim b$

- **Cooling capacity** depends on final field & magnetic moment strength
- When the cooling capacity is exhausted, the process has to
  be repeated again (**single cycle cooling**)

Cooling cycle

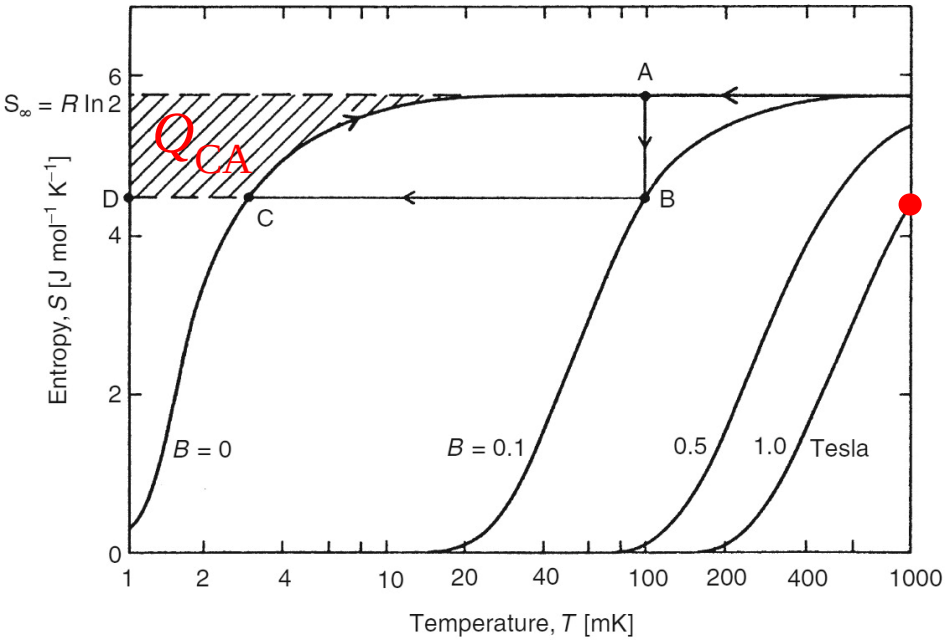

Fig. 9.1. Molar entropy of a single crystal of the paramagnetic salt CMN with angular momentum $J = 1/2$ (Sect. 9.4) as a function of temperature for magnetic fields applied along the cystallographic a axis. For the refrigeration process the salt is first isothermally magnetized (AB), and then after thermal isolation adiabatically demagnetized (BC). Eventually it warms up along the entropy curve at the final demagnetization field, which is zero in the example shown. The heat of magnetization during magnetization is given by the rectangle $ABDS_\infty$. The cooling power of the salt after demagnetization is given by the shaded area [9.4]

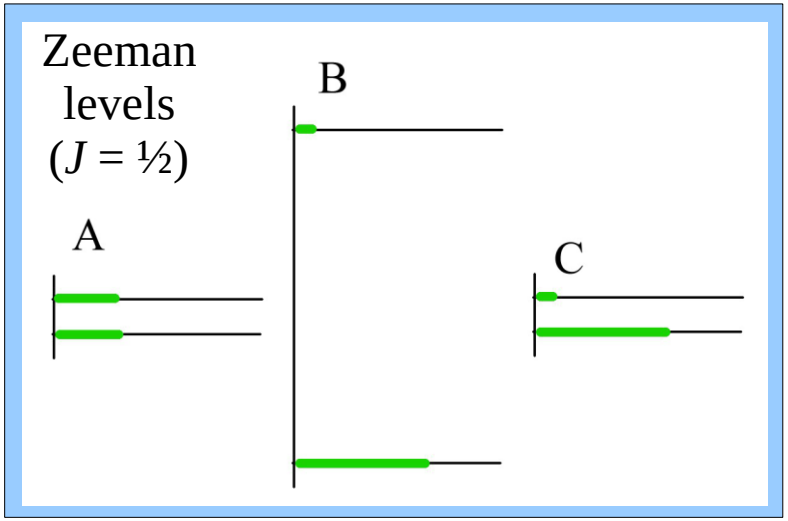

- Precool to point A: $B_{ext} = 0,\ T = T_i$
- Magnetize A → B,

  remove heat $Q_{AB} = T\Delta S$
- Isolate the system, $\Delta S = 0$ thereafter
- Demagnetize B → C
- Use the capacity C → A,

$$Q_{CA} = \int_{T_f}^{T} T\left(\frac{dS}{dT}\right)_B dT = \int_{T_f}^{T} C_B dT$$

$$Q_{CA} \ll Q_{AB}$$

Conventional magnetic refrigeration

- Uses paramagnetic salts (CMN, CPA, FAA, ...)
- Easy initial conditions $\boldsymbol{B_i = 1\ T}$ **and** $\boldsymbol{T_i = 1\ K}$ are sufficient
- **High cooling capacity** remains also at $B_{ext} = 0$
- Temperature can be measured from inherent property: $\chi = \lambda/T$
- **Fast,** demagnetization can be performed in few minutes

BUT

- **Poor thermal conductivity** limits heat transfer (**no electronic κ**)
- Difficult to mount samples (except liquid ^{3}He immersed in powdered CMN salt; 2 mK can be achieved)
- Single shot cooling

Largely replaced by dilution refrigerators

Space applications are still developed

Realizations

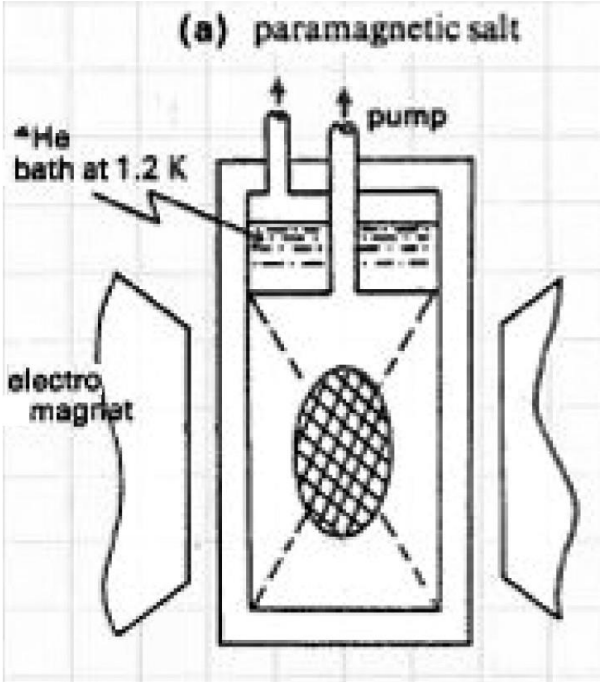

More elaborate schemes
with multiple stages producing
continuous refrigeration
from 4 K to mK-range
have been demonstrated

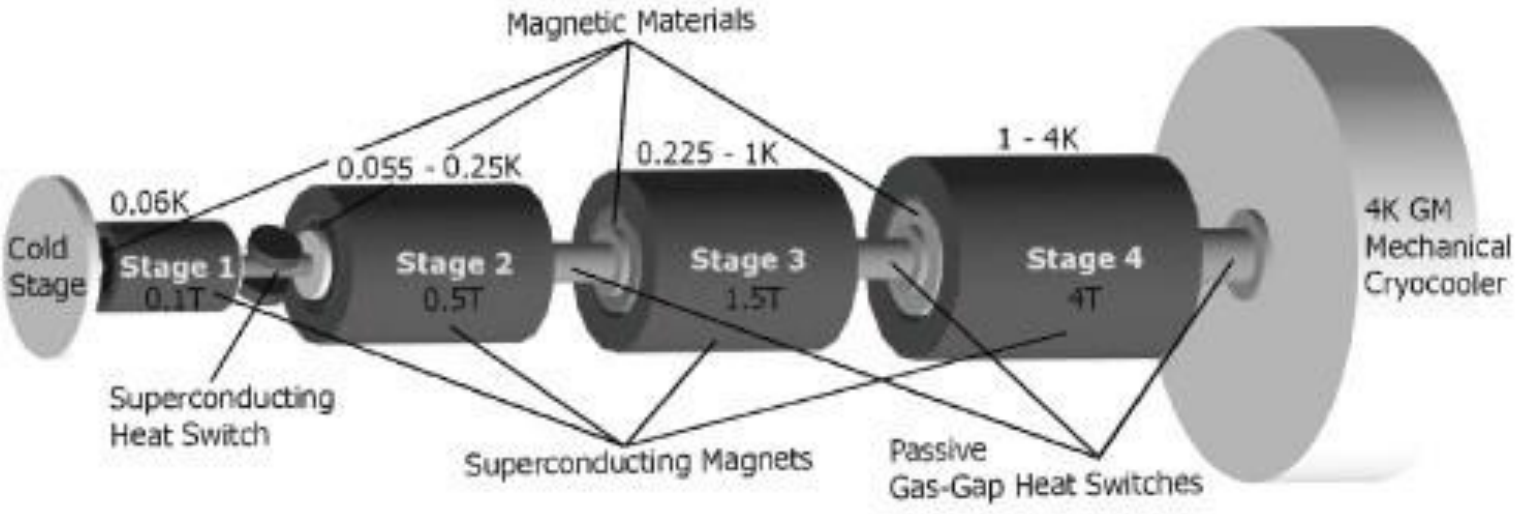

STAR CRYOELECTRONICS

Model DRC-200
ADR Cryostat

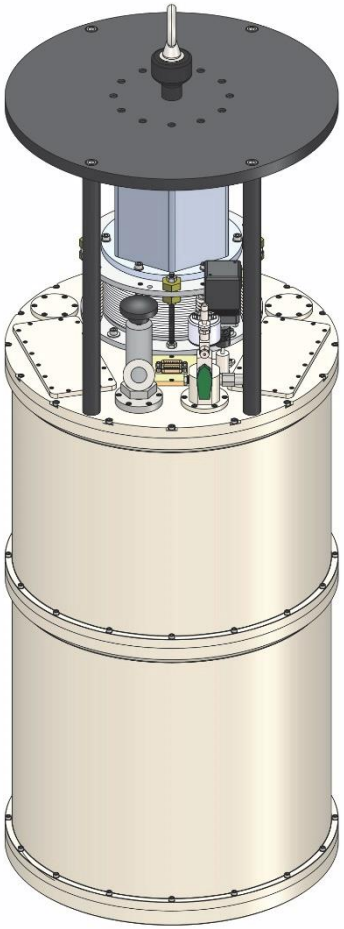

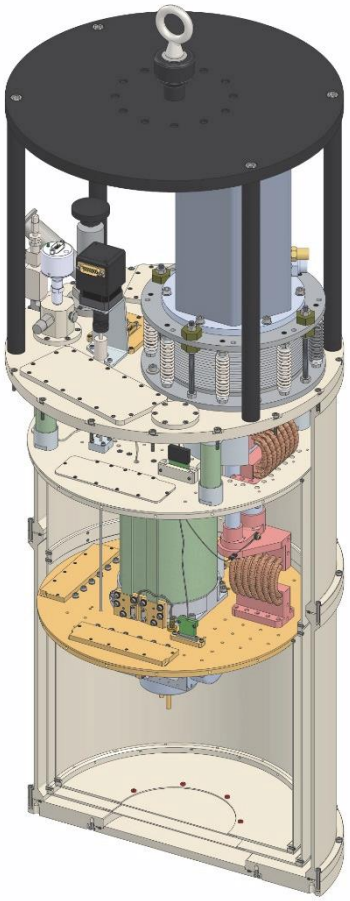

- Cryogen-free ADR design with 0.7 or 1 W pulse tube cooler.
- Fully automated ADR control and temperature regulation.
- Base temperature <50 mK, stability <5 μK_{rms} at 100 mK.
- Remote rotary valve and vibration isolation
  at 300 K, 60 K, and 3 K.
- Lightweight aluminum vacuum shells.
- Configurable with:
  TES or STJ X-ray detectors
  SQUID readouts, cryocables, custom IR filters

STAR CRYOELECTRONICS

Model DRC-200
ADR Cryostat

DRC-200 with GM cooler

Parameter	Value
Vacuum Jacket Size	41.9 cm diameter × 72.3 cm height
Weight	95 kg
Experimental Volume	33 cm diameter x 18 cm height
Primary Cooling Options	Cryomech PT-407 pulse tube cryocooler with remote valve, with CP2800 water-cooled compressor Sumitomo RP-082B2S pulse tube cryocooler with remote valve, F70 Series compressor
1st Stage Cooling Power	25 W at 55 K (PT-407), 35 W at 45 K (RP-082B2S)
2nd Stage Cooling Power	0.7 W at 4.2 K (PT-407), 0.9 W at 4.2 K (RP-082B2S)
Secondary Cooling	Two-stage ADR, GGG and FAA, 4 T superconducting magnet
GGG Cooling Capacity	1.2 J at 1 K
FAA Cooling Capacity	118 mJ at 100 mK
ADR Base Temperature	<50 mK
Hold Time	>150 hours regulation at 100 mK with no load
Temperature Control Range	Up to 250 mK
Temperature Stability	<5 μK_{rms} at 100 mK
Heat Switch	Automated
Pressure Monitoring	Pirani Gauge, atmosphere to 10^{-6} Torr
Electrical Feedthrough	DB-25 M, Magnet HDDB-26, Thermometry Two 25 mm Diameter Ports Two 152 mm x 55 mm Ports
Optional Accessories	Service stand; pump and vent manifold SQUIDs, cryocables, snout with detector arrays

ADR Kit for PPMS®

Quantum Design introduces a compact Adiabatic Demagnetization Refrigerator (ADR) designed for the PPMS platform as co-development work with the Institute for Materials Research, Tohoku University Japan. The ADR extends the PPMS temperature range down to <100 mK from room temperature in less than 3 hours, and holds temperature below 1.9 K for more than 2 hours. This enables DC resistivity and electrical transport measurements down to under 100 mK.

Features

- Extends the PPMS temperature range to < 100 mK in 3 hours
- Compatible with QD PPMS, EverCool II and DynaCool
- DC Resistivity and Electrical Transport measurements
- Two samples can be measured simultaneously
- Simple operation principle without mechanical movement

PPMS Requirements

- High vacuum option
- DC Resistivity (ETO puck)

Quantum Design

Preliminary Specification

Temperature range	300 K to 100 mK
Time to base temp	3 hours (from RT to <100 mK)
Temperature sensor	1000 Ω Ru_2O
Number of leads	8, allows for two samples to be measured simultaneously
Sample mounting	PPMS He^3 DC resistivity sample stage
System requirement	High vacuum option DC resistivity

ADR Process

1. Set sample puck in ADR and insert into PPMS
2. Cool down PPMS to 1.9K
3. Apply 3 T magnetic field
4. Vacuum PPMS to high-vacuum state
5. Set zero magnetic field
6. Temperature decreases to <100 mK

Temperature sweep data